

Nested Sampling for Non-Gaussian Inference in SLAM Factor Graphs

Qiangqiang Huang¹, Alan Papalia^{1,2}, and John J. Leonard¹

Abstract—We present nested sampling for factor graphs (NSFG), a novel nested sampling approach to approximate inference for posterior distributions expressed over factor-graphs. Performing such inference is a key step in simultaneous localization and mapping (SLAM). Although the Gaussian approximation often works well, in other more challenging SLAM situations, the posterior distribution is non-Gaussian and cannot be explicitly represented with standard distributions. Our technique applies to settings where the posterior distribution is substantially non-Gaussian (e.g., multi-modal) and thus needs a more expressive representation. NSFG exploits nested sampling methods to directly sample the posterior to represent the distribution without parametric density models. While nested sampling methods are known for their powerful capability in sampling multi-modal distributions, the application of the methods to SLAM factor graphs is not straightforward. NSFG leverages the structure of factor graphs to construct informative prior distributions which are efficiently sampled and provide notable computational benefits for nested sampling methods. We compare NSFG to state-of-the-art sampling approaches and Gaussian/non-Gaussian SLAM techniques in experiments. NSFG performs most robustly in describing non-Gaussian posteriors and computes solutions over an order of magnitude faster than other sampling approaches. We believe the primary value of NSFG is as a reference solution of posterior distributions, aiding offline accuracy evaluation of approximate distributions found by other SLAM algorithms.

I. INTRODUCTION

Simultaneous localization and mapping (SLAM), a fundamental problem in mobile robotics, is commonly posed as inferring the posterior distribution of robot and landmark states from relative measurements between the robots and landmarks. These posterior distributions are often expressed with factor graphs, which highlight the distribution’s conditional independence structure [1]. Precise distribution estimation of the posterior enables accurate uncertainty quantification for robust machine perception and lays a foundation for active perception tasks that require decision-making under uncertainty. Due to nonlinearities in real-world sensing models, the SLAM posterior is in general non-Gaussian. Exact inference over those non-Gaussian posteriors is generally intractable so practitioners resort to either deterministic or stochastic approximations.

In cases where the posterior distribution is sharply peaked at a single point in the state-space, it can be reasonable to approximate the distribution as Gaussian through the Laplace approximation [1]. However, the Laplace approximation cannot represent the highly non-Gaussian posteriors which arise in many SLAM problems due to circumstances such as range measurements, multi-modal data association or loop

Research supported by ONR grant N00014-18-1-2832, ONR MURI grant N00014-19-1-2571, and the MIT-Portugal program.

¹Computer Science and Artificial Intelligence Lab (CSAIL), Massachusetts Institute of Technology, 77 Massachusetts Ave, Cambridge MA 02139, USA {hq, apapalia, jleonard}@mit.edu

²Department of Applied Ocean Physics and Engineering, Woods Hole Oceanographic Institution, 86 Water St, Woods Hole, MA 02543, USA

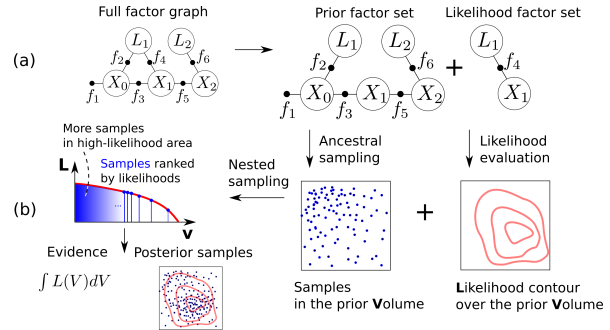


Fig. 1. Our approach to performing nested sampling over factor graphs. (a) The factor graph is first decomposed into two parts: a prior factor set and a likelihood factor set. (b) From the acyclic graph in the prior factor set we apply ancestral sampling to generate samples of the prior distribution. The functions for sampling and likelihood evaluation are supplied to a nested sampler. Nested sampling returns estimated evidence and samples which approximate the posterior distribution.

closure, and non-Gaussian noise models. Thus many non-Gaussian SLAM algorithms have been proposed to pursue a tractable but more expressive approximation of the non-Gaussian posterior.

Stochastic approximation algorithms, which represent the posterior distribution with samples, are generally recognized as more computationally expensive, but more expressive, inference solutions [1]. Our work falls into this class of algorithms. The resulting samples of these algorithms enable qualitative analysis of the posterior as well as estimation of statistical quantities of interest. Thus, stochastic approximation algorithms provide value in (1) offline accuracy evaluation of other algorithms and (2) high-fidelity posterior estimation for problems which do not require real-time results onboard a robotic system.

Nested sampling is a recent stochastic approximation technique that is powerful for sampling multi-modal distributions [2]. This work combines nested sampling with informative priors obtained from factor graphs. We term our algorithm nested sampling for factor graphs (NSFG). To the best of our knowledge, there are no existing general purpose algorithms for reference solutions even on posteriors of small SLAM problems. This need for accuracy evaluation motivated the development of NSFG, which pursues the *bona fide* shape of the posterior and thus aids accuracy evaluation of other SLAM inference algorithms.

NSFG is evaluated across four classes of simulated problems and a real-world dataset. Existing sampling approaches and state-of-the-art Gaussian/non-Gaussian SLAM algorithms are also compared. All implementations and experiments presented in this paper have been made freely available¹.

¹<https://github.com/MarineRoboticsGroup/nsfg>

II. RELATED WORK

There are two key aspects to our work: the use of the factor graphs to improve the underlying inference algorithm and the use of nested sampling to perform approximate stochastic inference. We will first survey inference techniques in SLAM with a focus on those leveraging factor graph structures. We will then discuss general stochastic inference techniques which have not yet been applied to SLAM.

A. Factor graphs and inference in SLAM

Factor graphs are a standard representation of SLAM problems which encode the conditional independence structure of the posterior distribution [3, 4]. This structure is commonly exploited to build efficient deterministic inference algorithms designed for near-Gaussian posteriors [5–9]. From these solutions the posterior distribution can be approximated as a Gaussian via the Laplace approximation [6, 10]. Other works extended the use of deterministic inference to conditions such as false data associations [11], multi-hypothesis estimation [12], and Gaussian mixtures [13]. NSFG differs from these methods, as it is sampling-based (i.e. stochastic inference) and does not assume any form on the posterior distribution.

Beyond deterministic inference, the SLAM community has explored stochastic inference techniques such as particle filtering [14–16] and Markov Chain Monte Carlo (MCMC) [17, 18]. Many particle filtering algorithms for SLAM (e.g., FastSLAM2.0 [16]) track landmarks by extended Kalman filters which cannot represent general non-Gaussian/multi-modal distributions. Recent work leveraged factor graphs and probabilistic modeling techniques such as non-parametric belief propagation [19, 20] and normalizing flows [21]. NSFG differs from these works in that it does not assume any parametric density models and builds upon a stochastic inference technique (i.e. nested sampling) which is generally more accurate for multi-modal distributions [22]. NSFG aims to improve inference fidelity at the cost of computational complexity. This tradeoff suggests that NSFG could be used in accuracy evaluation of approximate distributions found by SLAM techniques.

B. General stochastic inference techniques

Hamiltonian Monte Carlo (HMC) is an MCMC variant which guides sampling exploration with the gradient of the density function [23]. The No-U-Turn Sampler (NUTS) [24] extends HMC with automatic parameter tuning, improving usability and performance. However, multi-modal distributions with distant modes still pose general difficulties as state space exploration uses only local density information. Specialized MCMC algorithms designed for multi-modal distributions were recently developed [25, 26].

Sequential Monte Carlo (SMC) is a sampling algorithm which combines importance sampling, re-sampling, tempering, and MCMC. Particle filters in general are just special instances of SMC [27]. The use of tempering and MCMC alleviates sample impoverishment in standard particle filters (e.g., sampling importance resampling algorithms in [28, Alg. 4]). SMC usually requires a proposal distribution that possesses good coverage of the typical set of the target

density. It is difficult to design such a proposal distribution for a general high dimensional target density.

Nested sampling was proposed by Skilling [2] to compute the evidence or marginal likelihood for Bayesian inference with a by-product of posterior samples. It is mostly developed and used in the field of astronomy. Nested sampling has two attractive features: (1) well-defined stopping criteria related to the convergence of estimated evidence and (2) global exploration of the state space. Nested sampling (NS) methods keep exploring and drawing new samples from the state space until the estimate of evidence converges. NS has demonstrated great success with complex posterior distributions that possess multiple modes [29]. The practical benefits of NS methods include: (i) no predetermined number of samples and (ii) little to no tuning of proposal distributions is required to get accurate results. The estimated evidence by nested sampling is also helpful for model selection problems (e.g., multiple factor graphs under different data associations). There are several open-source nested sampling packages [22, 30, 31]. In particular, Speagle [22] developed dynesty, an open-source dynamic nested sampling package which our implementation of NSFG is built upon.

III. METHODS

We define the SLAM inference problem that NSFG solves, discuss nested sampling at a high level, and elaborate on how NSFG uses the conditional independence structure of factor graphs to improve the abilities of nested sampling.

A. Factor graphs and the problem formulation

We use the latent variable Θ to denote all robot poses (X) and landmark locations (L). Let z be all measurements. We aim to infer the posterior distribution of Θ given all measurements, i.e. $p(\Theta|z)$. The posterior distribution can be represented by a factor graph, as seen in Fig. 1a. A factor f_i represents a likelihood function over one or more variables which are denoted by Θ_i . We write the likelihood functions as $f_i(\Theta_i) = p(z_i|\Theta_i)$ in the case of measurements z_i and as $f_i(\Theta_i) = p(\Theta_i)$ in the case of prior distributions. The joint posterior then relates to our factors as follows, with m total factors in the graph:

$$p(\Theta|z) \propto p(z|\Theta)p(\Theta) = \prod_{i=1}^m f_i(\Theta_i) \quad (1)$$

B. Nested sampling

Nested sampling [2] was proposed to compute the evidence $p(z)$, with a by-product of posterior samples. The evidence is defined by an integral of the likelihood function $L(z|\Theta)$ and the prior distribution $\pi(\Theta)$ over the latent variable Θ , as seen in

$$p(z) = \int_{\Theta} L(\Theta)\pi(\Theta)d\Theta, \quad (2)$$

where $L(\Theta)$ stands for the likelihood $L(z|\Theta)$. In nested sampling, samples of Θ are drawn from the prior distribution. The prior distribution must cover all variables and is ideally computationally efficient to sample. The likelihood function contains the remaining factors of the posterior distribution.

Conceptually, nested sampling breaks up the sample space of the prior into *nested* areas. Each nested area is enclosed

by an iso-likelihood contour. We define the probability of a nested area as the prior volume $V \in [0, 1]$, while the likelihood on the contour is denoted by $L(V)$; thus, the small prior volume dV denotes the probability of a small iso-likelihood shell in the sample space. With the notion of prior volumes, nested sampling transforms the integration (2) to a one-dimensional integral of the likelihood over iso-likelihood small prior volumes, as follows [2, 29]:

$$p(z) = \int_0^1 L(V) dV. \quad (3)$$

In practice, each of the samples from the prior represents a small prior volume dV , and the sum of all small prior volumes is 1. Thus, the integration (3) can be implemented numerically by the likelihood-weighted sum of those prior volumes to estimate the evidence. To increase the precision of the numerical integration, nested sampling chooses to draw more samples from the prior volume where the likelihood is higher. This can be visualized using the V - L plot in Fig. 1b. Each bin under the V - L curve corresponds to a sample. The small prior volume and likelihood of a sample, respectively, determine the width and height of the bin. Those bins are ordered from left to right following a descending order of sample likelihoods (or bin heights). Thus, more samples naturally lead to finer bins that approach the theoretical V - L curve better.

Instead of drawing all samples of Θ only once from the prior distribution, nested sampling draws samples across iterations. With each iteration the feasible space of new samples gradually shrinks to high-likelihood areas in the sample space, leading to an efficient and accurate estimate of the evidence. This gradual focusing is often referred to as likelihood-restricted prior sampling (LRPS) [29], and is the most important step in nested sampling. We stress that LRPS is different from proposals in particle filters. While particle filters attempt to draw samples of a variable once from a proposal, the LRPS draws new samples across iterations until the estimated evidence converges; additionally, the weight of each sample depends on not only the likelihood but also the small prior volume. As the contribution of our work is not in performing nested sampling, but in using conditional independence structures from factor graphs to more efficiently prepare a problem for nested sampling, we refer interested readers to [2, 22, 29] for further details.

C. Nested sampling for factor graphs

1) *Proposed approach:* While nested sampling is a powerful approach to sampling complex distributions, naive application of nested sampling to SLAM does not take advantage of the conditional independence structure of SLAM. We focus on how to use this structure to enable nested sampling to be effectively applied to SLAM. Specifically, we exploit the sparsity structure of SLAM factor graphs to construct a prior $\pi(\Theta)$ and likelihood function $L(\Theta)$, which enhances nested sampling.

Factors in SLAM factor graphs usually consist of a few unary factors as priors, a number of binary factors modeling measurement likelihoods, and a few factors connected to a robot pose and multiple landmarks for modeling multi-model data association. As described in Section III-B, the

prior model for nested sampling, $\pi(\Theta)$, must be a tractable distribution from which samples of all latent variables can be efficiently drawn. Thus, $\pi(\Theta)$ must incorporate factors more than the nominal priors to cover all variables and, accordingly, these factors will be excluded from the likelihood model, $L(\Theta)$. We will introduce our strategy for selecting factors that compose $\pi(\Theta)$ and $L(\Theta)$.

Our strategy constructs a $\pi(\Theta)$ that enables ancestral sampling [1] for all variables, as ancestral sampling admits very efficient distributional sampling. NSFG effectively builds $\pi(\Theta)$ from a spanning tree, for trees naturally afford ancestral sampling.

NSFG assumes that any variable in the SLAM factor graph is connected to at least a binary factor (i.e., each variable is created along with a bivariate factor), implying that binary factors already form a connected graph of all variables. NSFG designates a node or variable connected to a prior factor as the root of the spanning tree. Starting from samples drawn from the prior factor for the root variable, one can use binary factors along the spanning tree to generate samples of descendant variables up to the leaves of the tree. As seen in Fig. 1a, we designate the factors involved in this ancestral sampling procedure as **PF** (prior factor set) and incorporate them in the prior model $\pi(\Theta)$ while the remaining factors are referred to as **LF** (likelihood factor set) and make up the likelihood model, $L(\Theta)$. The resulting factorization of the posterior distribution in (1) is

$$p(\Theta|z) \propto \underbrace{\prod_{f_j \in \mathbf{LF}} f_j(\Theta_j)}_{L(\Theta)} \underbrace{\prod_{f_i \in \mathbf{PF}} f_i(\Theta_i)}_{\pi(\Theta)}. \quad (4)$$

For example, for a typical SLAM factor graph with a single robot and K unknown landmarks, the **PF** set can be composed of the prior factor at the starting pose of the robot, odometry factors, and K binary factors that are connected to different landmarks. Notions such as the **PF** set have commonly been used in SLAM to initialize variables in MAP solvers and construct proposal distributions in particle filters. This work introduces such approaches to nested sampling, with a focus on sampling from joint posteriors in SLAM problems.

This partition of **PF** and **LF** sets improves nested sampling in two aspects: (i) the prior model resembles the posterior distribution better than simple proposals such as uniform distributions of all variables and (ii) the likelihood model involves fewer factors, which reduces the cost of likelihood evaluation in nested sampling. SLAM factor graphs are usually sparse, which implies that the cardinality of **PF** set can be comparable to or even much greater than the cardinality of **LF** set. Therefore, exploiting the sparsity structure of SLAM factor graphs can effectively improve both the computational performance and solution quality of nested sampling.

2) *Algorithms:* We implemented Algorithms 1 and 2 for obtaining the **PF** and **LF** sets and drawing posterior samples via NSFG. The factors in the **PF** set are constructed from a spanning tree, as seen in Algorithm 1, and are thus ordered for performing ancestral sampling. Note that selection of the prior factor for designating the root of the tree in line 3 of

Algorithm 1: Obtain PF and LF sets (spanning tree)

Input: Univariate factor set \mathcal{P} , binary factor set \mathcal{B} , and all other factors \mathcal{L}
Output: Prior factor queue **PF** and likelihood factor queue **LF**

- 1 Initialize empty FIFO queues of **PF** and **LF**
- 2 Construct a spanning tree \mathcal{T} from the graph formed by binary factors \mathcal{B}
- 3 Push a prior factor f from \mathcal{P} to **PF** and designate its variable as the root of \mathcal{T}
- 4 Traverse \mathcal{T} from the root to leaves and push binary factors to **PF** once they have been visited
- 5 Push all factors that are not in **PF** to **LF**
- 6 **return PF** and **LF**

Algorithm 2: NSFG

Input: Prior factor queue **PF** and likelihood factor queue **LF**
Output: Samples of the joint posterior distribution

Function *LLK*(latent variable Θ):

- 2 $l \leftarrow 0$ // Initialize log likelihood
- 3 **for** f in **LF** **do**
- 4 $l = l + f.\text{loglikelihood}(\Theta)$
- 5 **return** l

Function *PriorTrans*(hypercube sample \mathbf{u}):

- 7 Initialize a dictionary \mathcal{P} for containing prior samples
- 8 **for** f in **PF** **do** // Ancestral sampling in each iteration
- 9 $v \leftarrow$ Variable in f but not in \mathcal{P}
- 10 $\mathcal{P}[v] \leftarrow f.\text{hypercube_transform}(\mathbf{u}, \mathcal{P}, v)$
- 11 **return** \mathcal{P}

12 $\mathcal{S} \leftarrow \text{NestedSampling}(\text{PriorTrans}, \text{LLK})$

13 **return** \mathcal{S} // Return posterior samples

Algorithm 1 depends on user-defined heuristics (e.g., choosing a more informative prior). Using the **PF** and **LF** sets, Algorithm 2 defines the prior model $\pi(\Theta)$ and likelihood model $L(\Theta)$ that enable nested sampling. The likelihood model is simply evaluating the sum of the log-likelihoods of the factors in the **LF** set (line 1 in Algorithm 2). The use of the **PF** set for realizing $\pi(\Theta)$ is less straightforward since it involves density transformation (line 10 in Algorithm 2).

Nested sampling methods usually require transformation functions that map from the uniform distribution over unit hypercube to the prior distribution $\pi(\Theta)$, rather than explicit expressions of prior distributions [22, 29–31]. We refer to these transformations as hypercube transforms. Hypercube transforms are necessary because the unit hypercube is first sampled to enable global exploration of the state space. The transform applied to these samples casts the global exploration into the domain of the variable Θ , improving global coverage of the state space. Hypercube transforms can be implemented by quantile functions of noise models, which are available in typical SLAM problems (e.g., Gaussian noise models). With these hypercube transforms and observation models, we obtain samples for our first variable in the **PF** set and then apply ancestral sampling to propagate the samples along the tree encoded in the **PF** set (line 8 in Algorithm 2).

IV. IMPLEMENTATION

A. Observation and noise models

We introduce observation and noise models that will be used in our experiments. A noisy pose observation is defined by $\tilde{T} = T \exp(\xi^\wedge)$ where pose $T \in \text{SE}(d)$ is a

latent variable, \wedge turns ξ into a member of the Lie algebra $\mathfrak{se}(d)$, and $\xi \sim \mathcal{N}(\mathbf{0}, \Sigma)$ is the perturbation vector subject to a Gaussian distribution. A noisy range measurement is modeled by $\tilde{r} = \|\mathbf{t}_i - \mathbf{t}_j\|_2 + \mathcal{N}(0, \sigma^2) \in \mathbb{R}$ where \mathbf{t}_i is the translation component of variable X_i or L_i . Beyond binary factors with known data associations, we use sum-mixture factors to model ambiguous data association as follows

$$f_i(\Theta_i) = p(z_i|\Theta_i) = \sum_{j=1}^{|\mathcal{D}|} p(z_i|\Theta_i, d_j)p(d_j) \quad (5)$$

where each component is a binary factor with certain data association $d_j \in \mathcal{D}$. In our experiments we assume the data association prior $p(d_j)$ is a uniform distribution given no prior knowledge.

B. Other solvers for comparison

We use an open source package called *dynesty*, developed by Speagle [22], for performing nested sampling in line 12 of Algorithm 2. A vanilla sampler based on nested sampling was also implemented to justify the advantage of exploiting factor graph structure. In the vanilla sampler, all SLAM factors are incorporated into the likelihood model for nested sampling while predetermined uniform distributions of all variables are supplied as the prior distribution. This vanilla sampler is denoted as NS(UnifPr) in Section V for comparison.

Two other state-of-the-art stochastic inference methods, NUTS and SMC, a state-of-the-art Gaussian SLAM solver, GTSAM [32], and a non-Gaussian SLAM solver, NF-iSAM [21], are tested in our experiments as well. We supply our SLAM factors to the NUTS and SMC implementations in PyMC3 [33], GTSAM, and NF-iSAM to solve our SLAM problems. We used the default built-in initialization functions in PyMC3 for NUTS and provided a predetermined uniform distribution that covers the space of interest to SMC. The C++ library of GTSAM was used while all other techniques were implemented in Python. All computation was run on an AMD Ryzen ThreadRipper 3970X processor with 32 cores.

V. RESULTS

NSFG is evaluated across four simulated and one real-world dataset to observe different aspects of its performance and capability. The datasets are: pose-graph SLAM (Section V-A), range-only SLAM (Section V-B), sensor network localization (Section V-C), ambiguous data association (Section V-D), and the Plaza1 dataset (Sec. V-E). We emphasize that NSFG pursues high-fidelity samples of the posterior at the cost of computational complexity. While examples in this work are small-scale, they possess abundant non-Gaussian features in posteriors, warranting their potential as canonical examples for comparing algorithms in this work and validating efficient non-Gaussian inference techniques in the future.

Qualitative evaluation is performed by plotting the samples drawn by each inference algorithm. Points of different colors indicate different variables. We choose to compare the empirical mean, rather than the MAP point, of the samples with the ground truth to compute the RMSE. This choice was made for two reasons: (i) the MAP point among samples can be very random in posteriors with equally weighted modes,

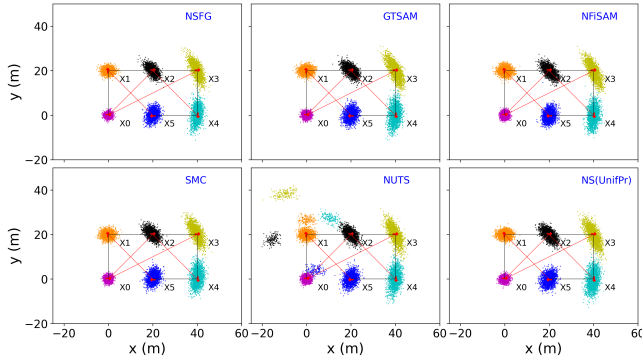


Fig. 2. Samples that represent estimated posterior distributions for a pose-graph with 6 poses (X0-X5) and 4 loop-closures. The robot starts in the lower left and travels counter-clockwise. The groundtruth poses are marked by arrows. The black lines indicate odometry measurements between successive poses. The red lines indicate loop closures. Samples are marked by colored dots, with different colors indicating different pose variables.

and (ii) the MAP point does not reflect secondary modes when gauging distributional errors.

A. Pose graphs

To test the simplest scenario in which all methods would be expected to work, we first evaluate 2D pose graphs. In Fig. 2 we show the results on one such problem. Samples of the GTSAM solution are drawn from the Laplace approximation provided by GTSAM. Estimated distributions by different methods were qualitatively similar with the exception of some spurious modes found in the NUTS solution.

Fig. 3 indicates that estimates made by the different samplers indeed converge as more samples are drawn. As a result of spurious modes shown in Fig. 2, the estimates by NUTS converge to different values from those by the other solvers. It is worth noting that estimated standard deviations of the x coordinate of X_4 by NSFG, SMC, NS(UnifPr), and NFiSAM converge to roughly the same value, but visibly differ from the GTSAM estimate. This difference is reasonable since the standard deviation estimated by GTSAM is a local Gaussian approximation at the MAP point of this non-Gaussian posterior.

For quantitative evaluation, Fig. 4a shows the root mean squared error (RMSE) and runtime of solutions for 10 randomly generated pose graphs with 10 poses. The runtime and accuracy of GTSAM are not plotted in Fig. 4a as GTSAM outperformed the RMSE and runtime of other approaches by several orders of magnitude on these pose graphs. Since the posteriors in these pose graphs are expected to be unimodal, a large RMSE in the figure is intended to indicate samples from spurious modes. Compared with the vanilla sampler relying on uniform prior distributions, NS(UnifPr), both accuracy and runtime performances are improved in NSFG. Notably, NSFG appears faster by a factor of 3-4. These results suggest the benefits of supplying an informative prior model to nested sampling. The narrow error bands for NSFG suggest that NSFG is more robust than other samplers.

B. Range-only SLAM

We evaluate range-only SLAM problems to explore performance on a simple, well-understood problem with non-Gaussian, multi-modal posterior distributions. We show a

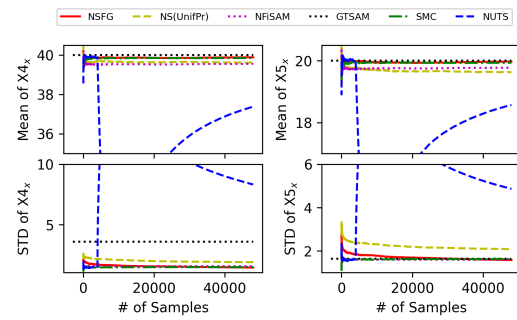


Fig. 3. Empirical mean and standard deviation over samples of x coordinates of selected variables (X_4 and X_5) in the pose graph example in Fig. 2. Note that samples generated in the burn-in and tuning stages of NUTS are discarded.

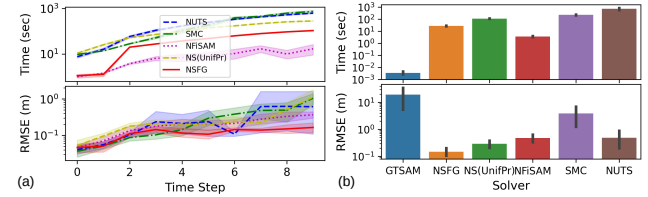


Fig. 4. Performance of different approaches in two experiments: (a) 10 randomly generated pose graphs with 30 dimensions each (10 poses), and (b) 10 randomly generated range-only SLAM problems with 14 dimensions (4 poses and 1 landmark position). Shaded areas in plot (a) and error bars in plot (b) indicate the 95% confidence interval.

single result from the range-only SLAM problems in Fig. 5. In the first three time steps (X0, X1, X2) the robot moves along a line, as such the posterior distribution of the landmark position consists of two distinct modes mirrored across the line driven by the robot. At the final time step (X3) the robot breaks away from the line, disambiguating the landmark position and causing the posterior distribution to converge to a single mode around the true landmark position. Qualitative evaluation of the solutions shows that NSFG best matches the expected posterior distribution for all time steps. This strongly suggests that NSFG can best approximate the posterior distribution of range-only SLAM problems.

In Fig. 4b we quantitatively compare all solvers on 10 other randomly generated range-only experiments. The statistics presented were computed at the final time step of each experiment after the distribution becomes unimodal (similar to time step 3 in Fig. 5). NSFG enjoys the lowest RMSE across different approaches. Note that in both pose-graph and range-only SLAM experiments, NSFG presents advantages over the other sampling techniques for accuracy and runtime (faster by over an order of magnitude in Fig. 4).

To explain the errors in SMC and NUTS, in Fig. 6 we display diagnostics explaining the issues observed in Fig. 5. As observed in the two plots on the right of Fig. 6, the MCMC chains are effectively stuck in local optima of the posterior. These local optima prevent the MCMC chains from mixing between the two modes of the distribution, leading to an incorrect estimate of weights over different modes. In the case of the NUTS solution at time step 2 (Fig. 5), all of the MCMC chains are stuck around a single mode, and are thus prevented from exploring and sampling the equally probable mirrored solution. In the case of the SMC solution at time step 3 (Fig. 5), since there is a local optimum around the spurious landmark position $L_{0,x} = 160$

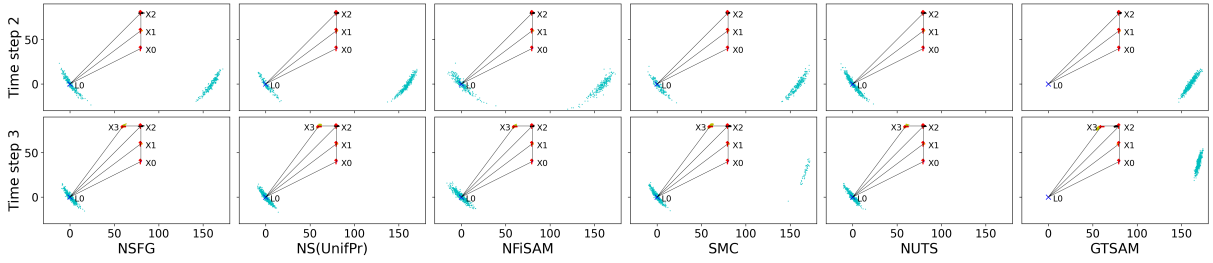


Fig. 5. Solutions generated by each of the inference methods for a range-only SLAM problem. The red arrows indicate the groundtruth robot pose and the blue points indicate samples of the estimated landmark state. The red and black lines denote range and odometry measurements, respectively. For the GTSAM solution, the initial value of the landmark L_0 is randomly picked on a circle that centers around the pose X_0 .

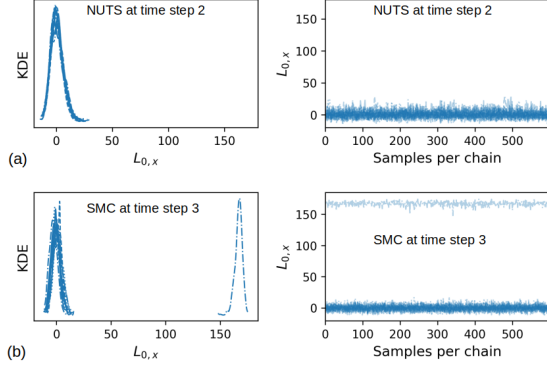


Fig. 6. Traces of the x-coordinate values of the landmark explored by the MCMC chains in Fig. 5 and kernel density estimation performed on the final distributions obtained from these MCMC chains. (a) NUTS solution for the baseline range-only problem at time step 2 and (b) SMC solution for the baseline range-only problem at time step 3.

which some MCMC chains cannot escape, samples from these chains incorrectly stress and overestimate the mode around the spurious landmark position.

C. Sensor network localization

To evaluate NSFG on a well-known non-Gaussian inference problem, we tested against the sensor network localization problem of [25]. The scenario and solution by NSFG are shown in Fig. 7. In brief, the inference goal is to estimate the posterior distributions of four unknown sensor locations, $\mathbf{t}_1, \dots, \mathbf{t}_4$, on the x - y plane provided two sensors with known locations, \mathbf{t}_5 and \mathbf{t}_6 , a few range measurements, $\{y_{ij}\}$, and a likelihood model. The measurement likelihood between sensors i and j is modeled as

$$f_{ij}(\mathbf{t}_i, \mathbf{t}_j | y_{ij}, w_{ij}) = \begin{cases} \exp\left(-\frac{\|\mathbf{t}_i - \mathbf{t}_j\|_2^2}{2 \times 0.3^2}\right) \exp\left(-\frac{(y_{ij} - \|\mathbf{t}_i - \mathbf{t}_j\|_2)^2}{2 \times 0.02^2}\right), & \text{if } w_{ij} = 1 \\ 1 - \exp\left(-\frac{\|\mathbf{t}_i - \mathbf{t}_j\|_2^2}{2 \times 0.3^2}\right), & \text{otherwise.} \end{cases}$$

where w_{ij} equals 1 if there is a distance measurement between sensors i and j otherwise it is zero. Thus the posterior for this example is

$$p(\mathbf{t}_1, \dots, \mathbf{t}_4 | \mathbf{y}, \mathbf{w}) \propto \prod_{\substack{i=2, \dots, 6 \\ j=1, \dots, 4 \\ i > j}} f_{ij}(\mathbf{t}_i, \mathbf{t}_j | y_{ij}, w_{ij}).$$

The scatter plots, histograms, and kernel density estimation in Fig. 7a and b highly resemble those in [25], further justifying the NSFG's ability to represent highly non-Gaussian posteriors.

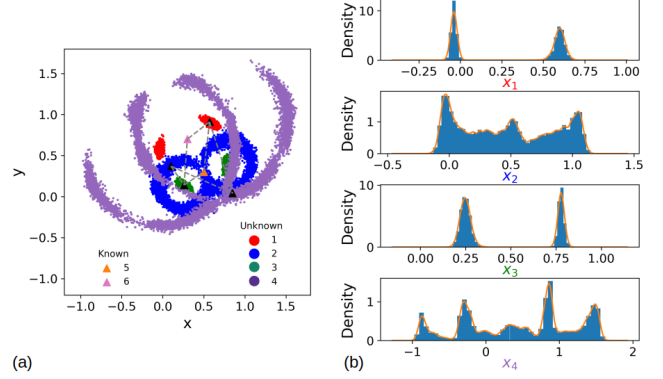


Fig. 7. Samples and corresponding histograms and kernel density estimation drawn by NSFG for the sensor network localization example in [25]. The four black triangular markers designate the groundtruth locations of four sensors whose positions are initially unknown. The two colored triangles designate the locations of two sensors at known locations. The dashed lines indicate range measurements from the various sensors to one another.

D. Range-only SLAM with ambiguous data association

In Figs. 8 and 9, we evaluate the performance of NSFG on a range-only SLAM problem with data association ambiguity. At time step 0, range measurements to two beacons are acquired with the identify information of beacons; from pose X_1 to X_4 , however, the landmark association is ambiguous (i.e. the robot is unsure of which landmark the distance measurement goes to). This class of problems was chosen as the posterior distribution is highly complex and demonstrates that NSFG can solve mixed continuous-discrete inference problems. In ground truth, L_1 is observed by X_1 and X_2 while X_3 and X_4 spot L_2 .

As seen in Fig. 8, NSFG displays the posterior distribution that arises from this situation and is capable of disambiguating the landmark locations by time step 7.

Alternatively, the posterior with data-association ambiguity can be represented with the following mixture model:

$$p(\Theta | z) = \sum_{i=1}^{|\mathcal{D}|} w_i p(\Theta | z, d_i), \quad (6)$$

$$w_i = \frac{p(z | d_i) p(d_i)}{\sum_{i=1}^{|\mathcal{D}|} p(z | d_i) p(d_i)}, \quad (7)$$

where \mathcal{D} denotes the set all data association combinations. Each mixture component stems from one of the data association hypotheses, i.e., $p(\Theta | z, d_i)$.

Fixing the data association for a given combination, d_i , results in a new posterior, $p(\Theta | z, d_i)$. For the new posterior,

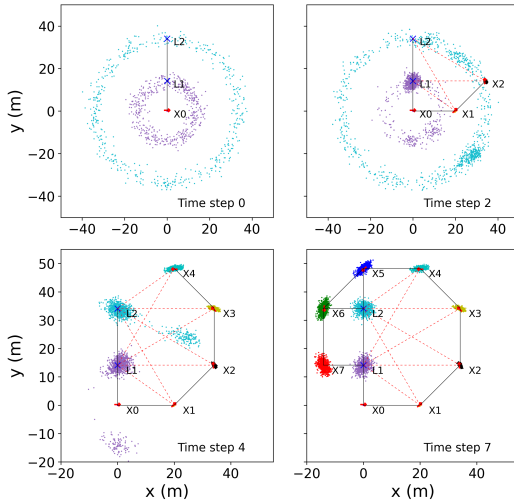


Fig. 8. Scatter plots for posteriors of a range-only SLAM problem with data association ambiguity using NSFG. The dashed red lines from the same robot pose (X) to multiple landmarks (L) denote a range measurement that can be associated with all these landmarks. Black lines denote measurements with known association.

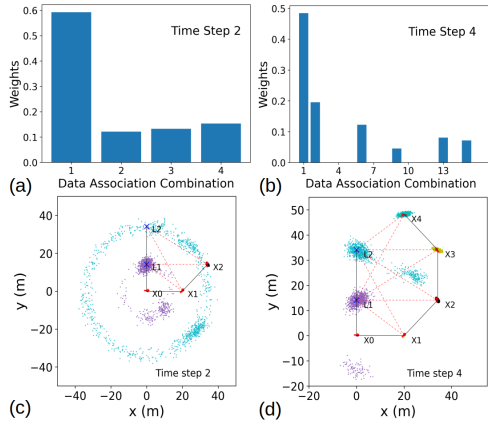


Fig. 9. Weights and posteriors under different data associations. (a) and (b) are estimated weights of data association hypotheses at time step 2 and 4 respectively. (c) and (d) are posterior samples formed by combining samples from individual components in Eq. (6).

NSFG can draw samples and estimate the evidence, $p(z|d_i)$. As there is no prior on data associations, $p(d_i)$ is assumed to be $\frac{1}{|D|}$. Thus, the weights of components in (6), w_i , can be computed if we apply NSFG to solve factor graphs resulted from all combinations of data association (Fig. 9, top). A new ensemble of samples representing the joint posterior can be formed by performing re-sampling over the samples and weights for different data associations, as seen in the bottom of Fig. 9. These scatter plots resemble their counterparts in Fig. 8 well. Effectively, this demonstrates that NSFG is self-consistent and can be used in multiple ways to reliably approximate complex posterior distributions.

E. Real-world dataset

We apply NSFG to solve early time steps in the Plaza1 dataset [34]. The dataset provides a sequence of timestamped odometry and range measurements collected by a mobile robot in a planar environment. The ranges were measured between the robot and four landmarks using ultra-wideband sensors for which a noise model can be found in [35]. We use measurements in the early stage of the sequence to create a

range-only SLAM factor graph. The factor graph involves 29 robot poses and 4 landmark locations, thus leading to a 95-dimensional posterior distribution at the final time step. The posterior distribution contains one prior factor, twenty-eight odometry factors, and thirty-three range factors. Additionally, we generate three more synthetic problems from this dataset which associate 20%, 40%, and 60% of range measurements with all landmarks. Such a range measurement with ambiguous data association (ADA) is modeled as a sum-mixture (5). These mixture factors are expected to incur a higher function evaluation cost than binary factors (a mixture factor entails evaluating 4 binary factors, given 4 landmarks here). We use these synthetic problems to investigate the impact of complex likelihood factor sets on the performance of NSFG.

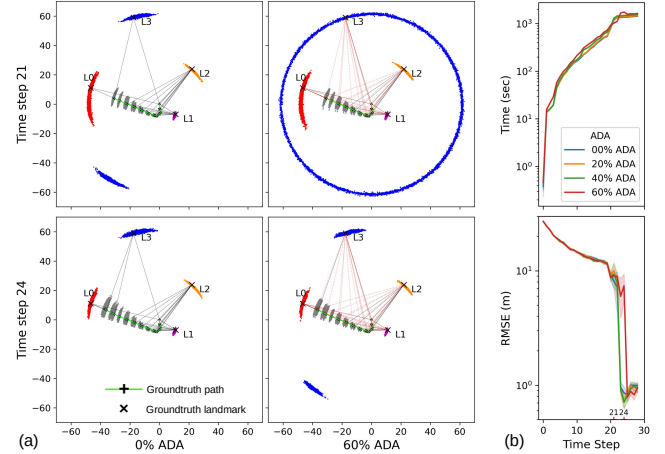


Fig. 10. Plaza1 dataset with different fractions of ADA: (a) posterior samples and (b) runtime and error. In plot (a), black lines indicate range measurements with known data association. Red lines from a robot pose indicate ambiguous range measurements. In (b), the shaded area indicates the 95% confidence interval estimated by six runs with different random seeds.

Fig. 10a shows samples drawn by NSFG at time steps 21 and 24. Given data association (0% ADA), we estimate that the posterior at time step 21 is dominated by two modes, which differ in the location of landmark $L3$; at time step 24, the posterior becomes unimodal. In contrast, the belief of landmark $L3$ becomes much more uncertain in the 60% ADA case. The RMSE in Fig. 10b supports this claim of distributional uncertainty. The transition from multimodal to unimodal posteriors sharply decreases the RMSE in all cases. However, such sharp reduction occurs to the 60% ADA case later than other cases. In the end of the sequence, the RMSE of 60% ADA converges to a low value, indicating the recovery of the groundtruth mode. As seen in Fig. 10b, more ADA factors incur greater computational cost, but these factors do not alter the scaling behavior of runtime with respect to dimensions. Note that later time steps entail more poses and greater dimensionality. In addition, we solve each of the factor graphs six times using different random seeds. The narrow error bands in Fig. 10b indicate that random seeds have little effect on NSFG.

We note that NSFG confirms that the joint posterior of landmarks and the robot path becomes peaked at a single point within the early time steps solved here. For the subsequent time steps in the dataset, one can confidently apply the

MAP estimation and (unimodal) Gaussian approximation to represent the joint posterior.

VI. CONCLUSION AND FUTURE WORK

We introduced nested sampling methods to directly draw samples from the posterior distributions encountered in non-Gaussian SLAM problems, pursuing the *bona fide* shape of the posterior. Leveraging the sparsity structure of SLAM factor graphs, our proposed approach, NSFG, provides nested sampling with informative prior distributions which can be efficiently sampled, leading to computational benefits for nested sampling methods.

We have demonstrated the advantage of NSFG over other sampling techniques and state-of-the-art Gaussian/non-Gaussian SLAM algorithms. NSFG presents superior robustness in inferring posteriors than all other approaches and operates over an order of magnitude faster than other sampling techniques. Additionally, we showed that the estimate of evidence, as a unique benefit of nested sampling, can be used to compute the posterior belief of ambiguous data associations, indicating the potential of NSFG for solving mixed continuous-discrete inference problems. Lastly, the performance of NSFG was demonstrated to be consistent under various conditions such as dimensionality, fractions of ambiguous data associations, and random seeding.

We believe that NSFG can be a promising tool for providing reference solutions for the posteriors in non-Gaussian SLAM problems. These solutions can aid accuracy evaluation of approximate inference algorithms and promote deeper understanding of uncertainty propagation on cyclic non-Gaussian SLAM factor graphs. Future work includes developing goodness-of-fit criteria of posterior samples for SLAM.

REFERENCES

- [1] Christopher M Bishop. "Pattern recognition and machine learning". In: Springer, 2006. Chap. 8, p. 365.
- [2] John Skilling et al. "Nested sampling for general Bayesian computation". In: *Bayesian analysis* 1.4 (2006), pp. 833–859.
- [3] Frank Dellaert, Michael Kaess, et al. "Factor graphs for robot perception". In: *Foundations and Trends® in Robotics* 6.1-2 (2017), pp. 1–139.
- [4] David M Rosen et al. "Advances in inference and representation for simultaneous localization and mapping". In: *Annual Review of Control, Robotics, and Autonomous Systems* 4 (2021), pp. 215–242.
- [5] Frank Dellaert and Michael Kaess. "Square Root SAM: Simultaneous localization and mapping via square root information smoothing". In: *The International Journal of Robotics Research* 25.12 (2006), pp. 1181–1203.
- [6] Michael Kaess, Ananth Ranganathan, and Frank Dellaert. "iSAM: Incremental smoothing and mapping". In: *IEEE Transactions on Robotics* 24.6 (2008), pp. 1365–1378.
- [7] M. Kaess et al. "iSAM2: Incremental Smoothing and Mapping with Fluid Relinearization and Incremental Variable Reordering". In: *IEEE Intl. Conf. on Robotics and Automation (ICRA)*. Shanghai, China, May 2011.
- [8] R. Kümmerle et al. "g2o: A General Framework for Graph Optimization". In: *IEEE Intl. Conf. on Robotics and Automation (ICRA)*. Shanghai, China, May 2011.
- [9] M. Kaess et al. "iSAM2: Incremental Smoothing and Mapping Using the Bayes Tree". In: *The International Journal of Robotics Research* 31 (2 Feb. 2012), pp. 217–236.
- [10] Michael Kaess and Frank Dellaert. "Covariance recovery from a square root information matrix for data association". In: *Robotics and autonomous systems* 57.12 (2009), pp. 1198–1210.
- [11] Niko Sunderhauf and Peter Protzel. "Switchable constraints for robust pose graph SLAM". In: *IEEE International Conference on Intelligent Robots and Systems* (2012), pp. 1879–1884.
- [12] Ming Hsiao and Michael Kaess. "MH-iSAM2: Multi-hypothesis iSAM using bayes tree and hypo-tree". In: *Proceedings - IEEE International Conference on Robotics and Automation* 2019-May (2019), pp. 1274–1280. ISSN: 10504729. DOI: 10.1109/ICRA.2019.8793854.
- [13] Tim Pfeifer, Sven Lange, and Peter Protzel. "Advancing Mixture Models for Least Squares Optimization". In: *IEEE Robotics and Automation Letters* 6.2 (2021), pp. 3941–3948.
- [14] J. González et al. "Mobile robot localization based on Ultra-Wide-Band ranging: A particle filter approach". In: *Robotics and Autonomous Systems* 57.5 (2009), pp. 496–507. ISSN: 09218890. DOI: 10.1016/j.robot.2008.10.022.
- [15] Jose-Luis Blanco, Javier González, and Juan-Antonio Fernández-Madriral. "Optimal filtering for non-parametric observation models: applications to localization and SLAM". In: *The International Journal of Robotics Research* 29.14 (2010), pp. 1726–1742.
- [16] Michael Montemerlo et al. "FastSLAM 2.0: An improved particle filtering algorithm for simultaneous localization and mapping that provably converges". In: *IJCAI*. 2003, pp. 1151–1156.
- [17] Roshan Shariff, András György, and Csaba Szepesvári. "Exploiting symmetries to construct efficient MCMC algorithms with an application to SLAM". In: *Artificial Intelligence and Statistics*. PMLR, 2015, pp. 866–874.
- [18] M. Kaess and F. Dellaert. "A Markov Chain Monte Carlo Approach to Closing the Loop in SLAM". In: *IEEE Intl. Conf. on Robotics and Automation (ICRA)*. Barcelona, Spain, Apr. 2005, pp. 645–650.
- [19] D. Fourie, J.J. Leonard, and M. Kaess. "A Nonparametric Belief Solution to the Bayes Tree". In: *IEEE/RSJ Intl. Conf. on Intelligent Robots and Systems, IROS*. Daejeon, Korea, Oct. 2016.
- [20] D. Fourie et al. "Towards real-time non-Gaussian SLAM for under-determined navigation". In: *2020 IEEE/RSJ International Conference on Intelligent Robots and Systems (IROS)*. Oct. 2020.
- [21] Qiangqiang Huang et al. "NF-iSAM: Incremental smoothing and mapping via normalizing flows". In: *2021 IEEE International Conference on Robotics and Automation (ICRA)*. IEEE, 2021, pp. 1095–1102.
- [22] Joshua S Speagle. "dynesty: a dynamic nested sampling package for estimating Bayesian posteriors and evidences". In: *Monthly Notices of the Royal Astronomical Society* 493.3 (2020), pp. 3132–3158.
- [23] Michael Betancourt. *A Conceptual Introduction to Hamiltonian Monte Carlo*. 2018. arXiv: 1701.02434 [stat.ME].
- [24] Matthew D Hoffman, Andrew Gelman, et al. "The No-U-Turn sampler: adaptively setting path lengths in Hamiltonian Monte Carlo". In: *J. Mach. Learn. Res.* 15.1 (2014), pp. 1593–1623.
- [25] Hyungsuk Tak, Xiao-Li Meng, and David A van Dyk. "A repelling-attracting Metropolis algorithm for multimodality". In: *Journal of Computational and Graphical Statistics* 27.3 (2018), pp. 479–490.
- [26] Emilia Pompe, Chris Holmes, and Krzysztof Łatuszyński. "A framework for adaptive MCMC targeting multimodal distributions". In: *The Annals of Statistics* 48.5 (2020), pp. 2930–2952.
- [27] Arnaud Doucet, Adam M Johansen, et al. "A tutorial on particle filtering and smoothing: Fifteen years later". In: *Handbook of nonlinear filtering* 12.656-704 (2009), p. 3.
- [28] M Sanjeev Arulampalam et al. "A tutorial on particle filters for online nonlinear/non-Gaussian Bayesian tracking". In: *IEEE Transactions on signal processing* 50.2 (2002), pp. 174–188.
- [29] Johannes Buchner. *Nested Sampling Methods*. 2021. arXiv: 2101.09675 [stat.CO].
- [30] F Feroz, MP Hobson, and M Bridges. "MultiNest: an efficient and robust Bayesian inference tool for cosmology and particle physics". In: *Monthly Notices of the Royal Astronomical Society* 398.4 (2009), pp. 1601–1614.
- [31] WJ Handley, MP Hobson, and AN Lasenby. "POLYCHORD: next-generation nested sampling". In: *Monthly Notices of the Royal Astronomical Society* 453.4 (2015), pp. 4384–4398.
- [32] Frank Dellaert. *Factor graphs and GTSAM: A hands-on introduction*. Tech. rep. Georgia Institute of Technology, 2012.
- [33] John Salvatier, Thomas V Wiecki, and Christopher Fonnesbeck. "Probabilistic programming in Python using PyMC3". In: *PeerJ Computer Science* 2 (2016), e55.
- [34] Joseph Djughash and Stephan Roth. "Navigating with Ranging Radars: Five Data Sets with Ground Truth". In: *Journal of Field Robotics* 26.9 (2009), pp. 689–695. DOI: 10.1002/rob. URL: <http://onlinelibrary.wiley.com/doi/10.1002/rob.21514/abstract>.
- [35] Qiangqiang Huang et al. "Incremental Non-Gaussian Inference for SLAM Using Normalizing Flows". In: *arXiv preprint arXiv:2110.00876* (2021).